minerals

Article

Estimating Perspectives of Oil and Gas in New Strata in the Southern and Surrounding Dayangshu Basin

Yanxu Liu [1], Yanling Lai [2,*], Wenyong Li [1], Feng Luo [1], Lijie Wang [3], Anqi Cao [1], Zhexin Jiang [4] and Shan Gao [1]

[1] China Aero Geophysical Survey and Remote Sensing Center for Nature Resources, Beijing 100083, China; liwenyong@mail.cgs.gov.cn (W.L.)
[2] Hebei Institute of Geological Environment Monitoring, Shijiazhuang 050021, China
[3] Oil and Gas Engineering Research Institute of Jilin Oilfield Company, Songyuan 138000, China
[4] College of Geoexploration Science and Technology, Jilin University, Changchun 130026, China
* Correspondence: a340191600@126.com; Tel.: +86-0311-69101682

Abstract: On the basis of elaborating on the regional geological background, this paper analyzes the lithological and sedimentary characteristics and explorative prospects of new strata with oil and gas in the southern and surrounding areas of Dayangshu Basin. Based on the latest high-precision airborne gravity and magnetic comprehensive survey data, combined with the latest data from geological explorations, physical surveys, and drilling, and the use of basin structure layering combination methods, we clarified the characteristics of the bottom of the Jurassic–Cretaceous and the occurrence characteristics of the Upper Paleozoic in the study area and revealed the determinative effect of multi-period structures on the most important sedimentary layers. Then, we summarized the accumulation conditions and prediction methods of hydrocarbons and proposed the oil and gas prospects of these deep new strata. The results show that the Liuhe Sag in Dayangshu Basin, the depression in the northeast of Longjiang Basin, and the northern parts of the Taikang swell have good source–reservoir–cap combination conditions and favorable structural characteristics for oil and gas, where there is a high potential for exploration.

Keywords: oil and gas; occurrence characteristics; airborne gravity and magnetism; new strata; exploration potential; Dayangshu Basin

Citation: Liu, Y.; Lai, Y.; Li, W.; Luo, F.; Wang, L.; Cao, A.; Jiang, Z.; Gao, S. Estimating Perspectives of Oil and Gas in New Strata in the Southern and Surrounding Dayangshu Basin. *Minerals* **2023**, *13*, 706. https://doi.org/10.3390/min13050706

Academic Editor: Paul Alexandre

Received: 8 March 2023
Revised: 24 April 2023
Accepted: 26 April 2023
Published: 22 May 2023

1. Introduction

The exploration of Dayangshu Basin began in the late 1950s. In the beginning, the purpose was to find coal and metal ores, and then oil and gas exploration began to be carried out. Due to the low level of exploration, the geological conditions relating to petroleum in the basin are not well understood, and only a preliminary understanding of the relevant geological issues is available. Additionally, the basin lacks airborne gravity data, and the airborne physical survey method is the most effective for sedimentary basin investigation. Previous aeromagnetic surveys suffer from scattered areas and inconsistent accuracy and measurement scales [1–11].

At present, the implementation of integrated aerial gravity and magnetic surveys has greatly enhanced the capabilities and application areas of aerial geophysical surveys [2,6,7,12]. In particular, a series of important results and steps have been made in the deep structural analysis of key oil and gas basins in China's onshore and offshore areas, and the lithological composition of tectonic layers, the controlling role of multi-phase tectonic stress fields in relation to sedimentary layers [13–16], and the distribution patterns of favorable oil- and gas-bearing structures [9,17–26].

Based on the newly collected high-precision airborne gravity and magnetic data, this paper reveals the lithological characteristics of new oil- and gas-bearing systems in the southern part of Dayangshu Basin, the spread pattern of deep new systems, the influence of multi-phase tectonics over sedimentary layers, and the characteristics of oil and gas reservoirs. The results provide a reference for the exploration of new oil- and gas-bearing formations in Dayangshu Basin and similar areas.

2. Regional Geological Background

2.1. Stratum

According to the ground outcrops and drilling data, the stratigraphy of the region can be seen from old to new in the Palaeoproterozoic, Lower Paleozoic, Upper Paleozoic, Triassic, Jurassic, Cretaceous, and Cenozoic (Figure 1).

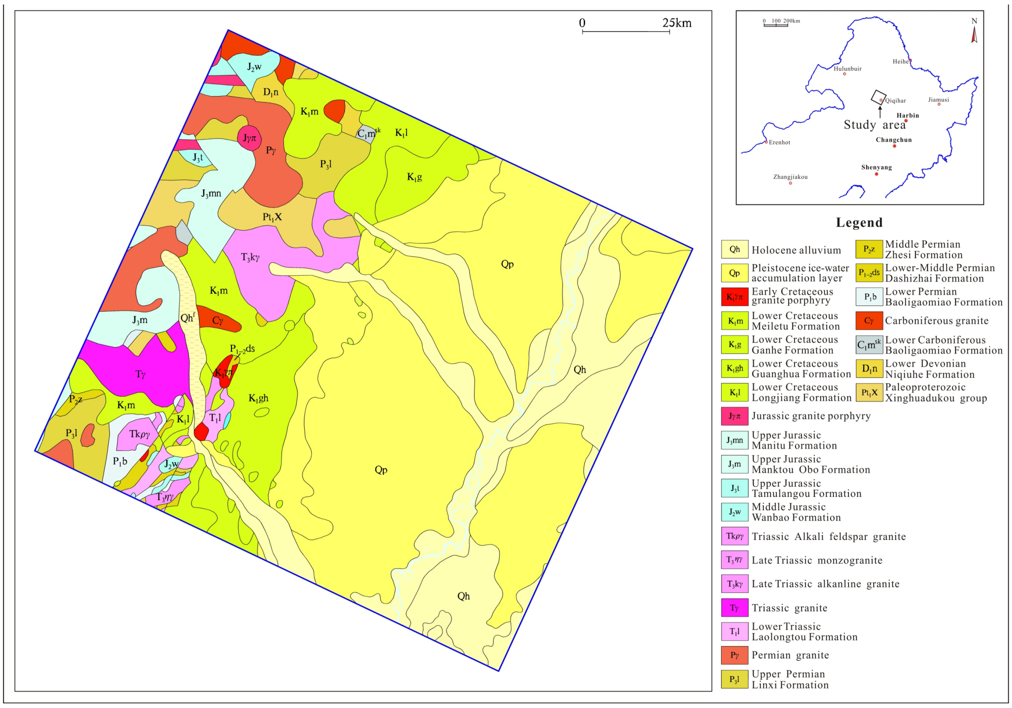

Figure 1. A geological map of the study area.

2.2. Regional Structural

With the exploration of regional geological structures and the revelation of deep structures, tectonic evolution played an important role in the analysis of crustal structures and the development of geological structures [6,10,15,27,28].

The western boundary of Dayangshu Basin is toward the Daxinganling supercrustal fault zone, and the eastern boundary is toward the western boundary of Songliao Basin. There are two nearly east–west crust faults across Dayangshu Basin near the Hailar-Jiayin and Boketu-Namur Riversand Dayangshu Basin is divided into three sections in the north–south direction. Among them, the Daxinganling fault zone, developed on the west side of Dayangshu Basin, has an important influence on the formation and evolution of Dayangshu Basin.

2.3. Regional Magmatic Rocks

According to the differences in formation environment, heterogeneity of fault activity, and different formation times, the size of magmatic rocks is quite different and the lithofacies and rock types are diverse. It even presents the landscape of a magmatic rock belt with specific spatial distribution rules. Magmatic activities often have important influences on regional tectonic history [29,30].

The magmatic activity in the study area and its periphery is very frequent, and it can be divided into five major cycles from old to new: Pre-Auranian, Garidonian, Hercynian, Yanshanian, and Xishanian, among which, the Hercynian and Yanshanian are the most intense. Both intrusive rocks and volcanic rocks are widely distributed. There are many kinds of intrusive rocks, including ultramafic, basic, neutral, acidic, and basic rocks; volcanic rocks are mainly acidic, neutral, and basic rocks.

3. Data and Methods

3.1. Aero Gravity and Magnetic Data

We use the comprehensive aeromagnetic measurements collected in 2018 by the China Natural Resources Airborne Physical Exploration and Remote Sensing Center in the southern part of Dayanshu Basin at a scale of 1:100,000, with a survey line direction of 115–295°, a cut line direction of 25–205°, and an average flight height of 175 m above ground. The total accuracy of spatial gravity measurements after data processing in the study area is 0.26×10^{-5} m/s^2, and the total accuracy of aeromagnetic measurement is 0.69 nT.

3.2. Physical Properties and Other Data

According to the distribution of stratigraphy and bedrock outcrop in the study area, the field survey completed 103 physical measurement points, obtained 3127 magnetization rate data, 435 density data, collected 454 specimens (including 8 magnetically oriented specimens); collected 5 seismic profiles, 3 boreholes, 2 geodetic electromagnetic bathymetric profiles, etc.

3.3. Constructing Layering Method

In this paper, based on aeromagnetic and gravity data, combined with the determination and analysis of stratigraphic density and magnetization rate parameters, different geophysical methods [31] are combined with seismic and drilling data as constraints, among which, the anomaly stripping method and Parker's iteration method are used for the depth of the Mesozoic bottom surface; the wavelet decomposition method is used for the regional gravity anomaly caused by the deep (mainly Moho surface) [32–37]; the calculated depth data are corrected with known drilling and seismic data as constraint control in the calculation process, and the thickness of the Upper Paleozoic and the depth of the Jurassic–Cretaceous bottom surface are obtained, respectively.

4. Oil and Gas Reservoir Characteristics of the Study Area

Based on the data of drilling and oil and gas exploration in Dayangshu Basin and nearby Longjiang Basin and Songliao Basin, this paper studies the geological conditions of these areas and surrounding areas as they relate to oil and gas, focusing on the source rock, reservoir, cap, and their combination, as well as the local structure and trap type.

4.1. Oil and Gas Source Rocks

The oil and gas source rocks in the study area, from top to bottom, mainly include the Upper Paleozoic Linxi Formation, the Dashiizhai Formation, the Zhezhi Formation, the Lower Cretaceous Ganhe Formation, the Jiufengshan Formation, and the Longjiang Formation.

4.1.1. Upper Paleozoic Oil and Gas Source Rocks

The Upper Permian and the Middle Permian all developed from dark mudstone. These dark mudstones show high organic matter abundance; the types of organic matter are mostly type II and type III, and the stage of evolution of this matter is high and mostly mature, meaning it has good oil and gas generation potential, and thus constitutes the main oil and gas source rocks in the region.

4.1.2. Lower Cretaceous Oil and Gas Source Rocks

The Ganhe Formation is mainly distributed in the depressional zone of Dayangshu Basin, and in the southern depressional zone, the stratigraphic thickness of the formation reaches over 2400 m. The maximum thickness of oil and gas source rocks in this formation reaches over 80 m, and it is thicker in the central part, becoming thinner toward the sides.

The Jiufengshan Formation developed in both the depression and uplift areas of the southern part of Dayangshu Basin; its thickness is relatively large in the depression area, reaching over 1000 m. The maximum thickness of oil and gas source rocks in the JiuFengshan Group is over 180 m, and the thicker strata of this group are distributed in the northeast of the Yang D1 well and the southwest of the Yang D2 well, with a trend of gradual thinning toward the sides.

The Longjiang Formation is mainly distributed in the southern depression of Dayangshu Basin, and then less so in the central and northern parts of the basin. The maximum thickness of oil and gas source rocks in the Longjiang Formation exceeds 40 m, and the thickest part of the formation is distributed in Dural and its southern area, south of the Yang D1 well and southeast of Dingjiatun.

The evaluation index of oil-bearing rocks indicates that all three sets of dark mudstone in the basin have oil- and gas-producing abilities, and the main oil and gas source rock is the Jiufeng Mountain Formation.

4.2. Reservoirs

The geological and geophysical data of the study area show that the Lower Cretaceous Longjiang, Jiufengshan, and Ganhe Formations have developed reservoirs. The Upper Paleozoic reservoir is found at the sea–land interface, where tuff and sandstone layers develop, and it mainly comprises sedimentary clastic rocks and fractured tuff.

4.3. Cover Layer

Dense volcanic lava, volcanic tuff, mudstone, and muddy siltstone have developed in the Longjiang, Jiufengshan, and Ganhe Formations in Dayangshu Basin, with dense rock structures and undeveloped pores and fissures, which together constitute the oil and gas cover of the basin.

5. Spatial Distribution Characteristics of the New Strata

5.1. Physical Characteristics of the New Strata

5.1.1. Density Characteristics

Regarding the variation in the formation's density, the formation extends from old to new, and its density generally ranges from large to small (Figure 2). The strata can be divided into three density layers, which are Proterozoic–Late Paleozoic, Mesozoic (Triassic, Jurassic, Cretaceous), and Cenozoic (Quaternary), listed from bottom to top. On the whole, the densities of volcanic rocks with different lithologies in the Jurassic–Cretaceous are obviously different. The density gradually increases from acid rock to intermediate acid rock, intermediate rock, and basic rock. The density of sedimentary rocks gradually decreases from the Proterozoic to the Paleozoic, Mesozoic, and Cenozoic.

Strata		Lithology	Number of specimens	Rock density (kg/m^3)
Cenozoic	Quaternary	Sandy soil	3	1960
		Clay	6	1950
Mesozoic	Cretaceous	Sand-mudstone、mudstone、sandstone、gritstone、conglomerate	29	2380
		Marlite	6	2410
		Tuffaceous sandstone	5	2490
		Rhyolite	10	2550
		Andesitic tuff 、dacite	25	2580
		Trachyte、trachyandesite、andesite	69	2550
		Basalt	26	2610
	Jurassic	Sandy mudstone、mudstone、siltstone、sandstone、conglomerate	109	2510
		Volcanic breccia	5	2450
		Tuffaceous sandstone	5	2410
		Rhyolitic tuff	10	2490
		Andesitic tuff 、dacite	27	2540
		Trachyandesite、andesite	26	2500
		Keratophyre	10	2620
		Basalt	3	2640
	Triassic	Siltstone、sandstone、glutenite	20	2530
Late Paleozoic	Permian	Mudstone、 sandstone	47	2600
		Limestone、 marlite	10	2660
		Andesitic tuff	7	2680
	Carboniferous	Mudstone、shale、sandstone	33	2630
		Dolomite、limestone	10	2690
	Devonian	Mudstone、shale、siltstone、sandstone、quartz sandstone、greywacke、glutenite	72	2630
		Dolomite、limestone、marlite	33	2750
		Schist、marble、granulite	19	2730
Early Paleozoic	Ordovician	Sandstone	5	2660
		Slate、schist、phyllite	15	2690
Proterozoic	Presinian	Amphibolite、schist、gneiss、phyllite、granulite	46	2760
		Migmatite	26	2730

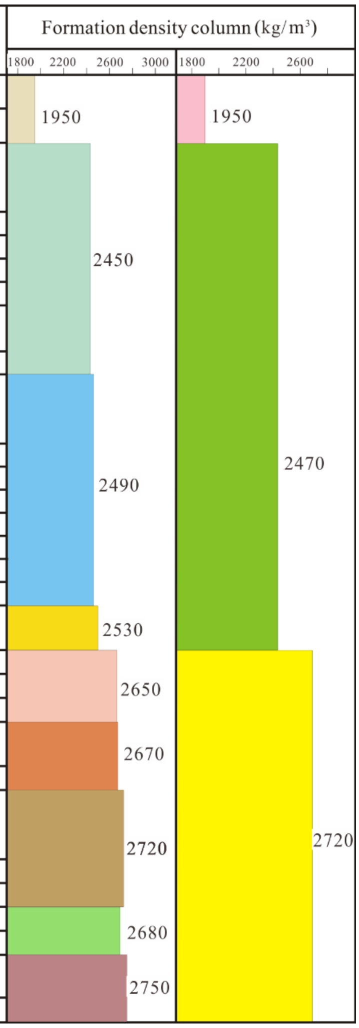

Figure 2. A density histogram of strata (rocks) in the study area and its surroundings.

5.1.2. Magnetic Characteristics

Regardings the magnetic difference, the magmatic rocks in the research area show strong magnetism, while the metamorphic rocks show weak magnetism, and the sedimentary rocks show the weakest magnetism (Figure 3). The main features include the following:

(1) The weak magnetic layer is mainly composed of sedimentary clastic rocks, and the average magnetic susceptibility is 30×10^{-5} SI, which does not cause obvious positive magnetic anomalies;

(2) The Cretaceous and Jurassic local distribution is a strongly magnetic layer, comprising thick but unstable intermediate–basic volcanic (clastic) rock types. Among these, the neutral volcanic rock's magnetism is greatly affected by lithology, and its magnetic susceptibility ranges from 1340 to 1867 $\times 10^{-5}$ SI. The average magnetic susceptibility of basic rock is 2052×10^{-5} SI, and this often causes high-amplitude jump changes that manifest positive magnetic anomalies;

(3) The Paleozoic regional distribution comprises a weak magnetic layer that is mainly composed of sedimentary rocks, with a magnetic susceptibility of less than 100×10^{-5} SI that does not cause obvious positive magnetic anomalies;

(4) The Proterozoic medium-strong magnetic layer comprises a set of medium-strength magnetic metamorphic rock series, which cause certain gentle-amplitude positive magnetic anomalies.

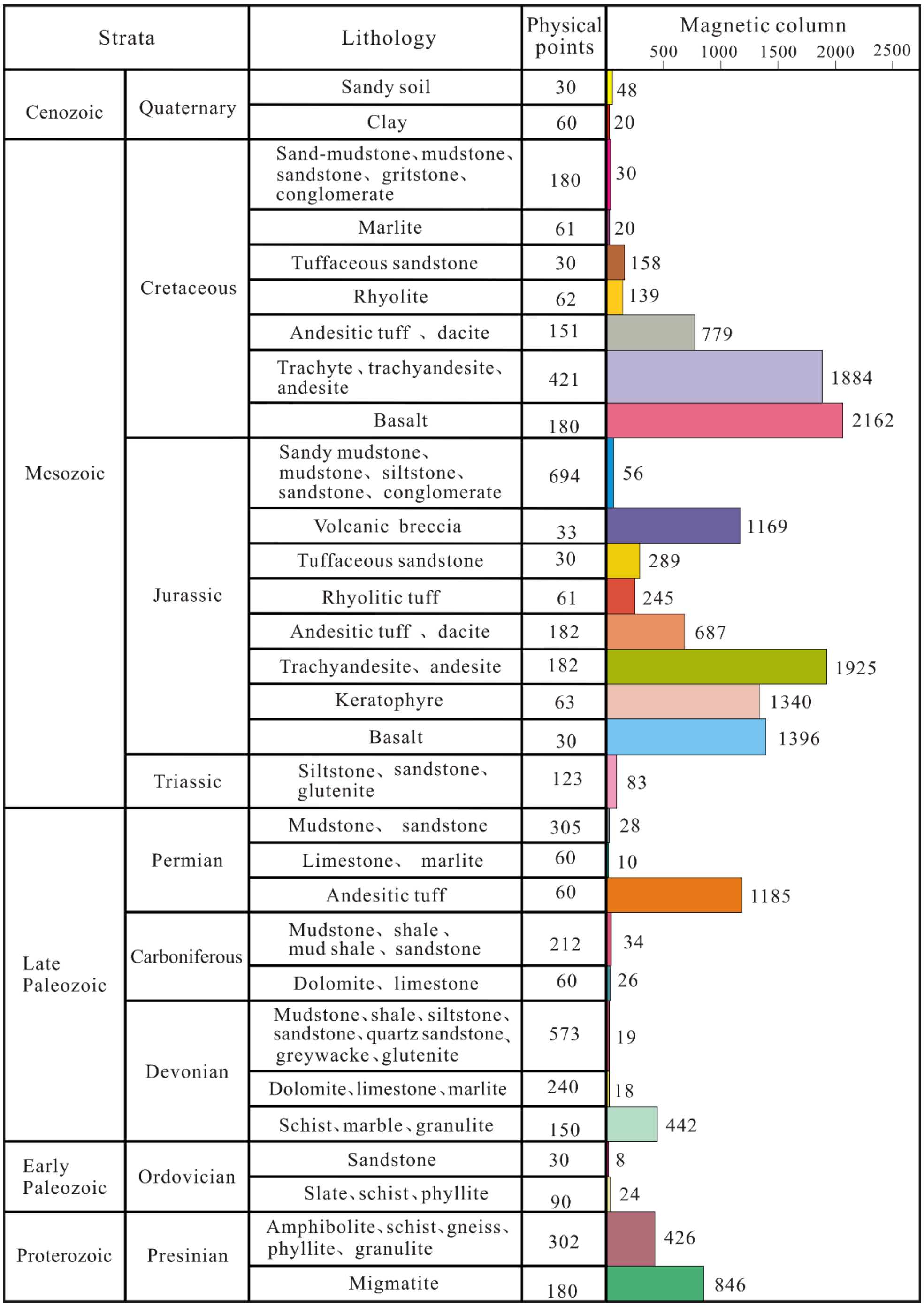

Figure 3. A magnetic susceptibility map of strata (rocks) in the study area and its surroundings.

5.2. Occurrence Characteristics of Deep New Strata

5.2.1. Upper Paleozoic Spreading Characteristics

Since the classic target layer of oil and gas exploration is the Mesozoic, there are relatively few data or results related to exploration in the deeper layers of the Upper Paleozoic, whether from drilling or seismic exploration. The thickness of the Upper Paleozoic has been calculated, and a thickness contour map has been drawn (Figure 4). It can be seen that the Upper Paleozoic in the study area has the following characteristics:

(1) The Upper Paleozoic boundary mainly developed in the central and eastern parts of the study area, while the thickness of the Upper Paleozoic boundary in the western part of the study area is small and locally missing;

(2) The thickness of the Upper Paleozoic boundary varies from 0 to 6000 m, and the development stage of the Upper Paleozoic boundary in different tectonic units varies significantly. The Upper Paleozoic boundary in the northern Dayangshu Basin is buried at a greater depth, and an obvious center of thickness can be seen in the northwest corner of the Pingyang Terrane (the thickness of the center is greater than 6000 m), which gradually increases as one moves from the surrounding terrane to the center. The depth of the central and south-central Longjiang Basin is about 2000–6000 m, and the three centers of thickness are located in the northeast and southeast of Longjiang Basin (the thickness value of the center is greater than 6000 m). The eastern part of the study area (the western slope of Songliao Basin) also shows a thickness characteristic of the Upper Paleozoic, and the thickness of deposition here is relatively stable, mostly around 3500–5000 m;

(3) A series of thickness gradient zones have developed in the Upper Paleozoic, such as in the central and western parts of the study area where the thickness gradient is dense, and the distribution of the Upper Paleozoic is obviously controlled by the NWW-oriented F3 fracture. In the eastern part of the south of the study area, the Upper Paleozoic thickness gradient zone near the southern section of the F_1 fracture is more apparent, and the thicknesses of the upper and lower plates of the fracture vary significantly, indicating that the fracture structure controls the development of the Upper Paleozoic in this region;

(4) In the same zone, the thickness of the Upper Paleozoic is relatively stable, without obvious local jump changes.

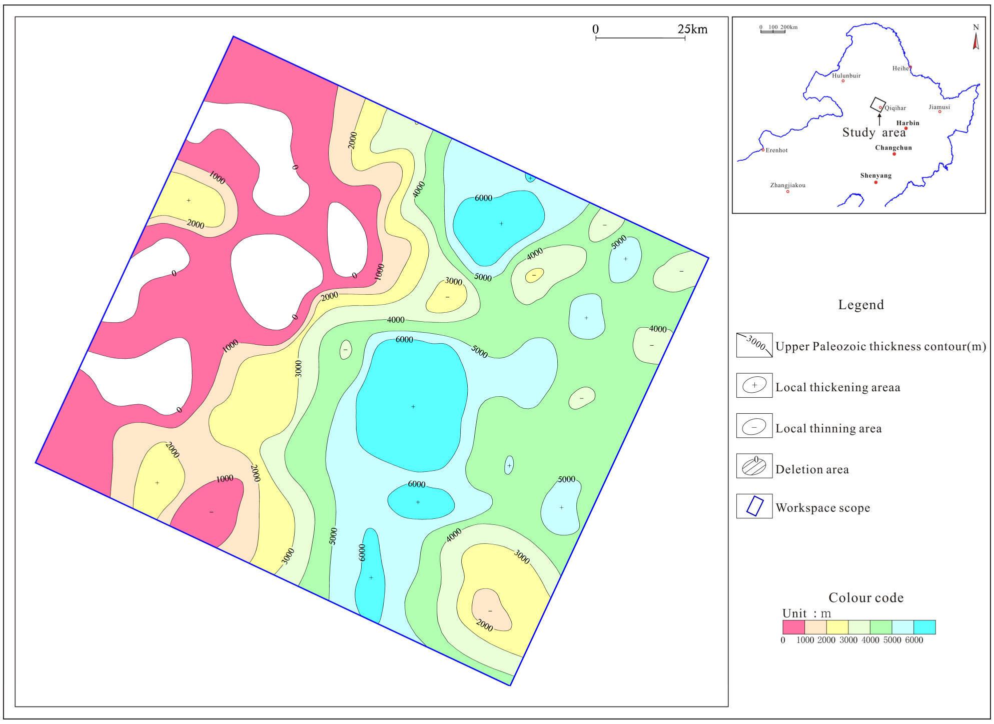

Figure 4. The thickness of the Upper Paleozoic in the study area.

5.2.2. Jurassic–Cretaceous Spreading Characteristics

Drilling and seismic data regarding the density of this set of strata locate them between the Cenozoic and pre-Jurassic strata. The characteristic features of the Jurassic–Cretaceous stratigraphic development in the study area are obvious (Figure 5).

(1) Jurassic–Cretaceous stratigraphy is more developed.

It is preserved in several tectonic units in the northern, south-central, and eastern parts of the study area. In the west, the strata set is missing in most areas.

(2) Jurassic–Cretaceous thickness zoning is obvious.

The thickness of the whole region varies from 0 to 3000 m and is greater in the central and southern parts. The thickness of the Mesozoic boundary in the western slope of Songliao Basin gradually increases from west to east, while the thickness of this boundary in the western Guangfeng Bulge and the western part of the southern Taikang Bulge is mostly 500–1500 m. The Mesozoic boundary in the eastern depressions is relatively thick, and its maximum depth exceeds 2000 m.

(3) The Mesozoic bottom surface has distinct depth centers. They are at the northeast and southwest of the Liuhe Sag, the south of the Pingyang Terrane, the northeast and northwest of the northeastern depression of Longjiang Basin, the Shanquan Depression, the Fufu Depression, the gentle slope zone of the Heping Farm, the eastern part of the Yantongtun Depression, and the southwest of the Taikang Bulge, for a total of 10 depth centers.

(4) Jurassic–Cretaceous depression boundaries are mostly fractured structures. For example, the Jurassic–Cretaceous system that has developed in the Liuhe Sag of Dayanshu Basin is sandwiched between the F_{24} fault, the F_{25} fault, and the F_{26} fault, and the distribution of the Mesozoic boundary in this region is obviously controlled by the fault structure.

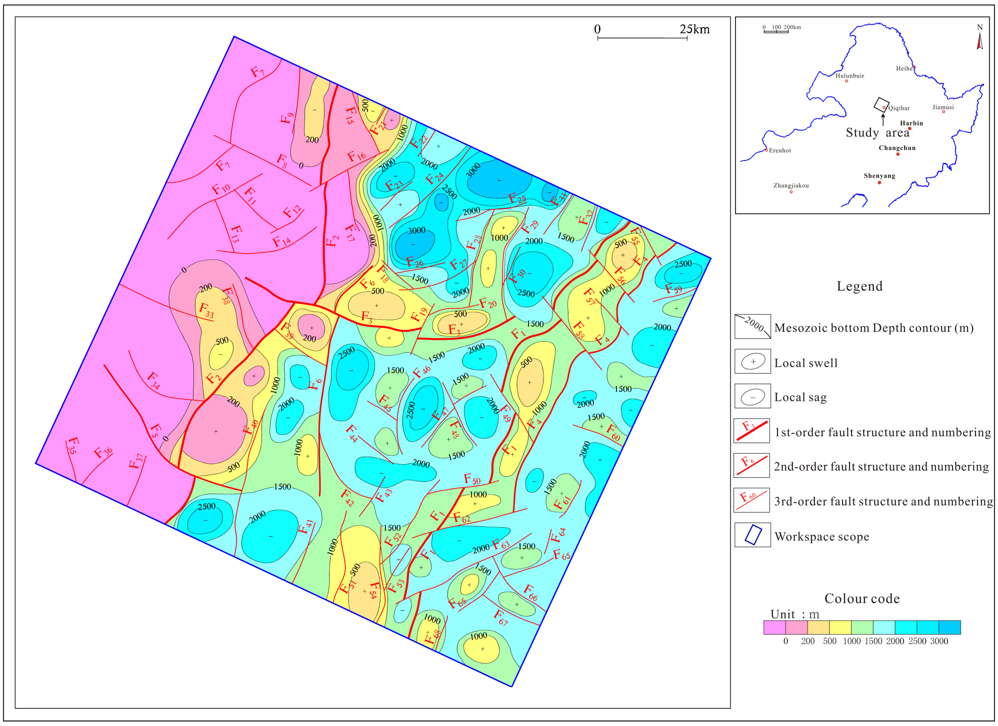

Figure 5. A bottom depth map of the Jurassic–Cretaceous system in the study area.

6. Oil and Gas Exploration Potential

6.1. Evaluation Methodology

Here, based on the Mesozoic and Upper Paleozoic ranges and their thicknesses, as illustrated by airborne gravity and magnetic data, combined with known drilling data, the prospective oil- and gas-bearing conditions in the study area were comparatively evaluated on the basis of production, storage, and cover combinations, as well as oil and gas transport, accumulation, and preservation conditions, and two categories of prospective oil and gas zones were delineated.

6.2. *Division of Prospective Oil- and Gas-Bearing Areas*

6.2.1. The Class I Prospective Oil- and Gas-Bearing Areas

The Class I prospective oil- and gas-bearing areas are the most favorable for oil and gas enrichment, and the most promising for oil and gas transport and gathering units in the study area. These areas are located in the western part of Dayangshu Basin, the eastern part of Longjiang Basin, and the southern part of the western slope of Songliao Basin, respectively. They contain three prospective oil- and gas-bearing areas, including Liouhe, Harakhai North, and Taikang (Figure 6).

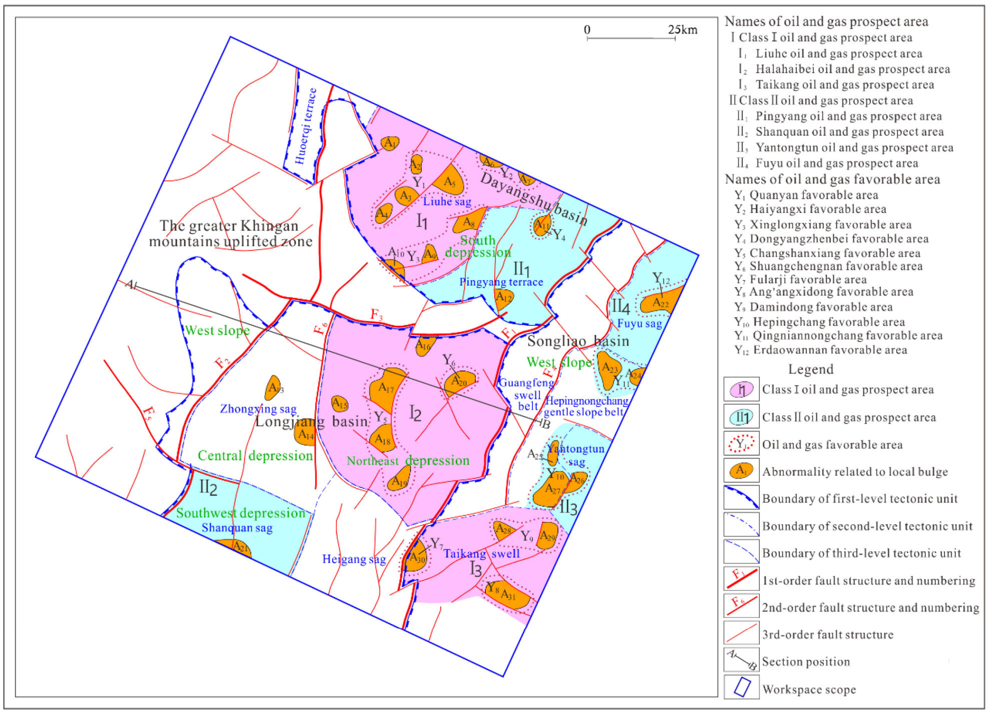

Figure 6. Prospective prediction of oil and gas in the study area.

(1) The Liuhe prospective oil- and gas-bearing area basically corresponds to the Liuhe Sag in the western part of Dayangshu Basin, which covers a large area of about 1660 km^2 and is the main oil and gas generation and transport area in the region of interest. A Mesoproterozoic boundary of a certain thickness has been deposited in this area. In addition, the Upper Paleozoic boundary, with a thickness of about 1000–6000 m, is also deposited in this prospective area. Vertically speaking, this prospective area has a good configuration of raw reservoir and cover. Across the plane, there are sufficient oil and gas sources in the area, and the data on the parameter wells in the area show that oil and gas are visible here. In addition, a series of local high-gravity anomalies are apparent in the interior of the Liuhe Sag, mainly in the central, northwestern, and southern areas. These local high-gravity anomalies are mostly local structures within the depression, which provide good conditions for oil and gas accumulation and preservation.

(2) The prospective oil- and gas-bearing area of Harahay North is located in the central part of the study area, which basically corresponds to the northeastern depression of Longjiang Basin, with an area of about 2403 km^2, and also has good conditions for oil and gas generation and transportation. The thickness of the Mesozoic boundary deposited in this area is relatively stable, with a varied range of about 1500–2500 m. Five Mesozoic depth centers can be seen in the prospective area, located in the northeast, center, southwest, and northwest of the prospective area. The aerial Bouguer gravity vertical one-guide anomaly map and the remaining anomaly map of the area show several local anomalies of small amplitude, which indicate storage sites in the

northeastern depression with sufficient oil and gas sources. The geomagnetic profile shows that this low-gravity and low-magnetic area is basically consistent with the distribution range of the larger low-resistance body (Figures 7–9). It is inferred that this area represents a relatively stable and continuous sedimentary depression, and the local gravity anomalies (Figure 8a–d) that have developed within the depression reflect the development of local structures, such as low swells and fault noses. The aeromagnetic anomaly maps and the related upward continuation maps (Figure 8e,f) indicate that the magmatic activity in this area is weaker compared to the surrounding area. A large range of negative magnetic anomalies indicates that a certain thickness of weakly magnetic sedimentary strata has developed in this area.

(3) The Taikang prospective oil- and gas-bearing area is located in the southeast corner of the study area, roughly corresponding to the north-central part of the Taikang Bulge on the western slope of Songliao Basin. The depth of the Mesozoic boundary in this prospective area is mostly 1000–2000 m, with relatively little variation, and the depth center is located in the northwest. In addition to the Mesozoic boundary, an Upper Paleozoic boundary of a certain thickness also developed in this area. The thickness of the Upper Paleozoic boundary gradually increases from the southeast to the northwest. The local anomalies are mainly distributed in the northeast, southeast and western parts of the area, and can provide a place for oil and gas storage. Drilling data for the area show that local industrial oil flow has been registered.

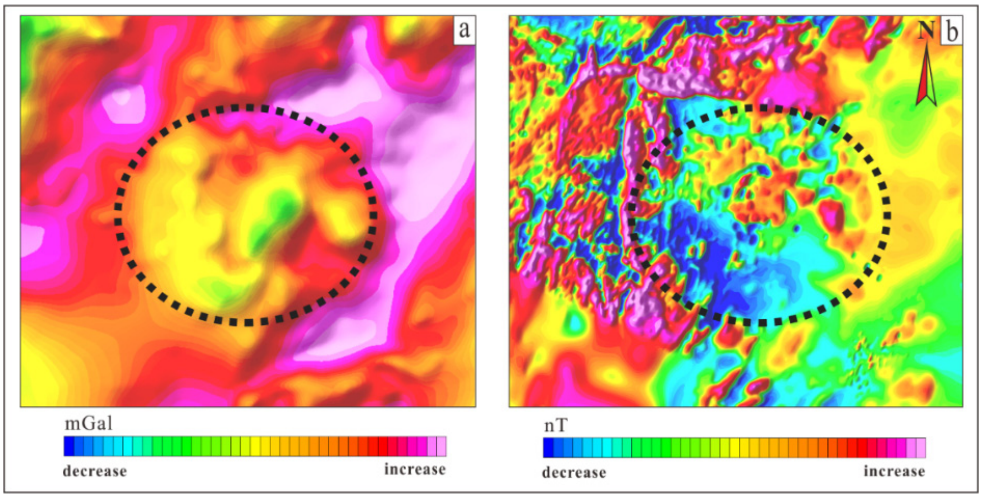

Figure 7. (**a**) A three-dimensional shadow map of the airborne gravity anomaly in the northeastern depression of Longjiang Basin; (**b**) a three-dimensional shadow map of the airborne magnetic anomaly in the northeastern depression of Longjiang Basin.

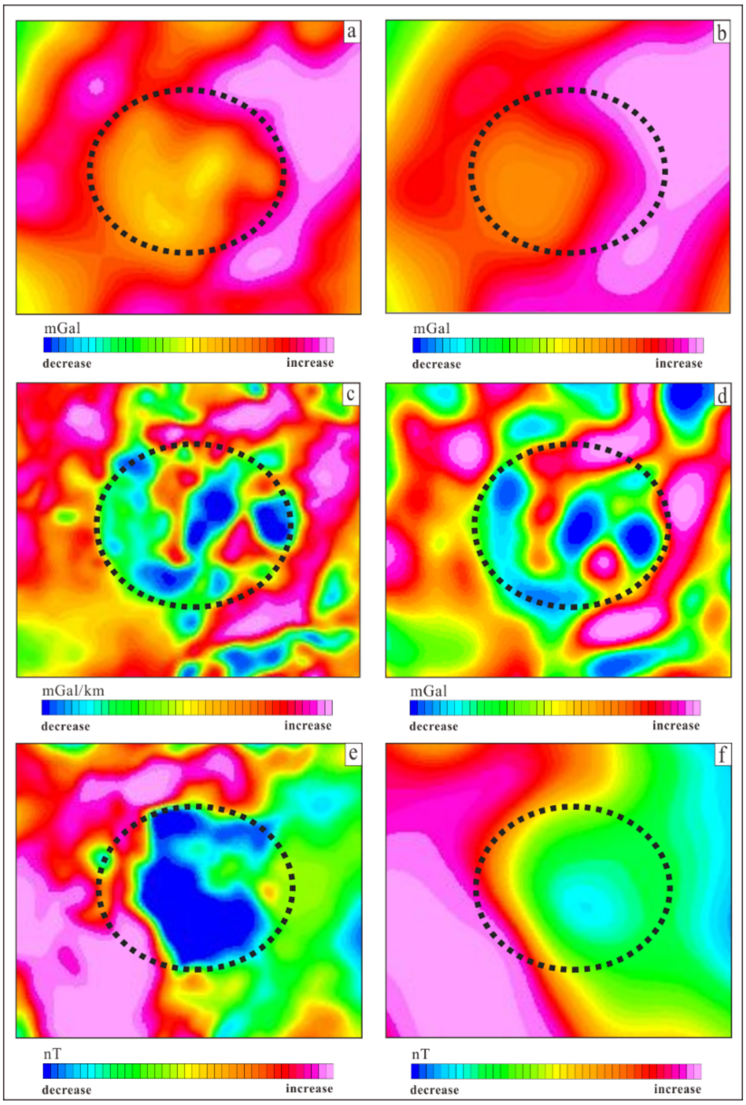

Figure 8. (**a**) Airborne Bouguer gravity anomaly extends upward for 3 km; (**b**) airborne Bouguer gravity anomaly extends upward for 15 km; (**c**) a vertical derivative map of airborne Bouguer gravity anomaly; (**d**) airborne Bouguer gravity residual anomaly; (**e**) airborne magnetic anomaly extends upward for 3 km; (**f**) airborne magnetic anomaly extends upward for 15 km.

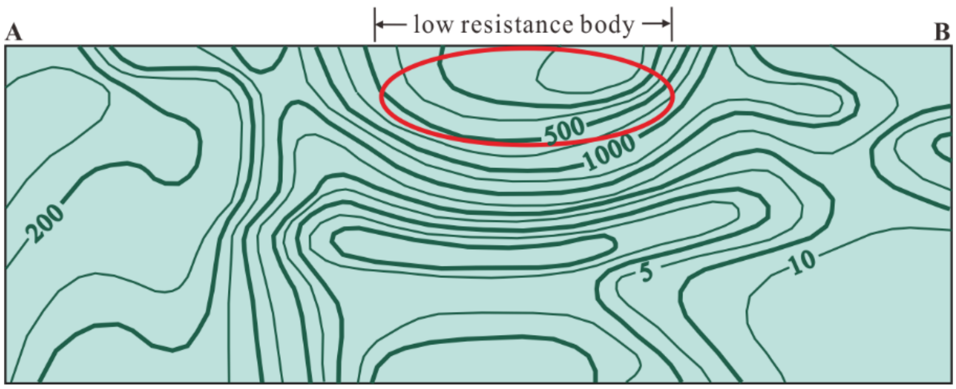

Figure 9. Geomagnetic bathymetric profile (over the northeastern depression of Longjiang Basin. The range in the red circle refers to low resistance body). AB: Section position shown in Figure 6.

6.2.2. The Class II Prospective Oil- and Gas-Bearing Areas

Class II prospective oil- and gas-bearing areas refer to the more oil- and gas-rich regions in the study area, the secondary oil- and gas-bearing and aggregating regions in the study area, or the areas that are closer to effective oil- and gas-bearing depressions, and which show certain prospects for oil and gas exploration. These are mainly located in the eastern part of Dayangshu Basin, the northern and central parts of the western slope of Songliao Basin, and the southern and western parts of Longjiang Basin.

(1) The prospective oil- and gas-bearing area of Pingyang is located in the southern part of Dayangshu Basin, which basically corresponds to the Pingyang Terrace and covers an area of 1110 km^2. The Mesozoic boundary is more developed here, and has been deposited at a thickness of about 1500–2500 m. An obvious center of thickness can be seen in the southwest, with a maximum thickness value of more than 2500 m. The area also shows characteristics of the Upper Paleozoic, with a thickness value of about 3000–6000 m, and its maximum thickness (more than 6000 m) is detected in the northwest corner of Pingyang Terrace. A certain number of local anomalies have developed in the prospective area. The area is well-configured, with good reservoir cover, and should have good oil and gas prospects.

(2) The Shanquan oil- and gas-bearing prospective area corresponds to the Shanquan Depression in Longjiang Basin, with an area of about 714 km^2. The Mesozoic boundary here is relatively developed, with a thickness of about 1500–2500 m, which is relatively stable. In addition, an Upper Paleozoic boundary of a certain thickness also developed in this prospective area, and the thickness of sediment here is about 1000–3000 m, showing a trend of gradually increasing from the northwest to the southeast. The reservoir cover in the area is well-configured, and it should have good oil and gas prospects.

(3) The Yantongtun oil- and gas-bearing prospective area corresponds to the Yantongtun Depression and its western side. The two tectonic units contained in the area have deposited a Mesozoic boundary of a certain thickness—about 1500–2000 m. In addition, an Upper Paleozoic boundary with a thickness of about 4500–5000 m has also developed in this area. Its thickness center is located in the transition area between Yantongtun Depression and the gentle slope of Heping Farm. The Mesozoic and Upper Paleozoic boundaries are relatively thick and have a good reservoir cover configuration, which should yield good oil and gas prospects. According to the latest information derived from airborne physical prospecting, the Shenyang Geological Survey Center has implemented heavy, magnetic, electric, seismic, and drilling work in this prospect area, and encountered a Carboniferous–Permian system at 1370 m.

7. Conclusions

(1) The Liuhe Sag in Dayangshu Basin, the northeastern depression in Longjiang Basin, and the northern part of the Taikang Bulge show good conditions for production, storage, and cover. The results of comprehensive high-precision airborne gravity and magnetic studies show that a series of local high-gravity anomalies have developed in the prospective area, and these anomalies mainly reflect the existence of bedrock bumps, including bedrock backslopes, subduction hills, and broken noses. These are mostly favorable local structures within the depressions and provide good sites for oil and gas accumulation and preservation. The new deep oil- and gas-bearing formations show a certain thickness and extension in the vertical direction; in the plane, the parameter data of wells in the Liuhe Sag and Taikang Bulge show that oil and gas have been found, and high-precision airborne heavy magnetic data combined with electrical, seismic, and drilling data have recently shown that the northeast depression of Longjiang Basin has low weight, low magnetism, and low resistance. The Mesozoic Depression is thus characterized by the “three lows”.

(2) Using a combination of data conversion and processing, we can further reveal the spatial spreading pattern, tectonic control factors, main lithological composition, oil and

gas reservoir, and oil- and gas-bearing new formation system based on the analysis of oil and gas geological conditions in the study area. In this study, the thickness of the Upper Paleozoic and the depth of the Jurassic–Cretaceous base were calculated for the first time by using high-precision airborne gravity and magnetic inversion, which indicates that not only the Jurassic–Cretaceous (thickness 0–3250 m, mostly 1000–2500 m) but also the Upper Paleozoic (thickness 0–6500 m, mostly 2000–6000 m) are developed in the study area.

(3) Based on the latest measured large-area high-precision aeromagnetic data, the favorable structural parts of new oil- and gas-bearing systems can be quickly screened. The high-precision aeromagnetic survey, combined with drilling, seismic, and electrical methods, and other auxiliary means, is one of the important ways to achieve an accurate, rapid, and efficient search for oil and gas resources.

Author Contributions: Data curation, Investigation, Writing—original draft, and Writing—review & editing, Y.L. (Yanxu Liu), Y.L. (Yanling Lai) and W.L.; Writing—review & editing, F.L., L.W., A.C., Z.J. and S.G. All authors have read and agreed to the published version of the manuscript.

Funding: This work was supported by the Geological Survey Project of China Geological Survey (No. DD20190028), the Geological Exploration Foundation Project of Hebei of China (No. 300012000000224097), and the Geological Survey Project of China Geological Survey (No. 1212011220563 and No. 12120114090401).

Data Availability Statement: Not applicable.

Conflicts of Interest: The authors declare no conflict of interest.

References

1. Xing, J.S.; Yang, W.R.; Xing, Z.Y. Deep-seated structure characteristics of eastern China and its relation with metal mineralization-concentrated region. *Earth Sci. Front.* **2007**, *14*, 114.
2. Li, W.Y.; Zhou, J.X.; Zhou, X.H.; Guo, Z.; An, Z.; Xu, J.; Li, B. Geological-genetic classification and prospecting significance on local anomaly of airborne gravimetry. *Adv. Earth Sci.* **2010**, *25*, 1061–1069.
3. Zhao, Z.K.; Jiang, T.; He, J.L. The oil and gas exploration prospect of Carboniferous—Permian in Songliao basin, northeastern China. *Geol. Bull. China* **2011**, *30*, 221–227.
4. Li, W.Y.; Zhou, J.X.; Xiong, S.Q.; Guo, Z.; Lu, W.; Xu, J.; Liu, Y. Effect and prospect of basic geological survey based on airborne gravimetry in China. *Acta Geol. Sin. Engl. Ed.* **2012**, *86*, 38–47.
5. Zhu, R.K.; Zou, J.X.; Mao, Z.G. Characteristics and distribution of continental tight oil in China. *J. Asian Earth Sci.* **2019**, *178*, 37–51. [CrossRef]
6. Li, W.Y.; Liu, Y.X.; Xu, J.C. Onshore Offshore Structure and Hydrocarbon Potential of the South Yellow Sea. *J. Asian Earth Sci.* **2014**, *90*, 127–136. [CrossRef]
7. Liu, Y.X.; Li, W.Y. Interpretation of Local Anomalies of airborne gravity in the south yellow sea. *Prog. Geophys.* **2015**, *30*, 418–1425.
8. Du, J.H. Analysis of natural gas accumulation conditions and exploration perspective in the central paleo-uplift belt (north), Songliao basin. *China Pet. Explor.* **2017**, *22*, 1.
9. Liu, Y.X.; Li, W.Y.; Cao, A.Q. Recognition of Tuquan basin structure based airborne gravity magnetic characteristics. *Geol. Surv. China* **2018**, *5*, 44–50.
10. Guo, Q.L.; Wang, S.J.; Chen, X.M. Assessment on tight oil resources in major basins in China. *J. Asian Earth Sci.* **2019**, *178*, 52–63. [CrossRef]
11. He, D.F.; Ma, Y.S.; Liu, B.; Cai, X.; Zhang, Y.; Zhang, J. Main advances and key Issues for deep-seated exploration in petroliferous basins in China. *Earth Sci. Front.* **2019**, *26*, 1–12.
12. Liu, Y.X.; Li, W.Y.; Xu, J.C. The utilizaion of wavelet magnitude method of gravity anomaly in fault identification. *Geophys. Geochem. Explor.* **2014**, *38*, 96–99.
13. Zhang, X.; Zhao, L.; Liu, T.Y.; Yang, Y.S. Multi—Scale wavelet separation of aeromagnetic anomaly and study of faults in Beijing area. *Acta Seismol. Sin.* **2006**, *19*, 542–551. [CrossRef]
14. Liu, Y.X.; Li, W.Y.; Yang, D.H.; Lu, W.F.; Wang, S.M. Study on characteristics of aeromagnetic anomaly and prospecting in Tuchengzi, northwest Hebei province. *Prog. Geophys.* **2019**, *34*, 2301–2308.
15. Jiang, W.L.; Tian, T.; Chen, Y.; Wang, X.; Zhang, J. Detailed crustal structures and seismotectonic environment surrounding the Su-lu segment of the Tan-lu fault zone in the eastern China mainland. *Geosci. J.* **2020**, *24*, 557–574. [CrossRef]
16. Li, W.Y.; Liu, Y.X.; Lu, W.F.; Ma, G.Q.; Zhang, C.S.; Zhao, J.W. Characteristics of Zhangsanying-tongshanzi aeromagnetic anomaly zone and prospecting potential of iron deposits in northern Hebei, China. *Glob. Geol.* **2020**, *23*, 99–115.
17. Achim, B.; Jia, J.L.; Susanne, A.I.S. Palaeo environmental conditions during deposition of the Upper Cretaceous oil shale sequences in the Songliao basin (NE China): Implications from geochemical analysis. *Org. Geochem.* **2012**, *46*, 76–95.

18. Wang, S.Y.; Cheng, Y.H.; Zeng, L.; Miao, P.; Jin, R.; Zhang, T.; Li, C.; Zhang, X. Thermal imprints of Cenozoic tectonic evolution in the Songliao basin, NE China: Evidence from apatite fission-track (AFT) of CCSD-SK1 borehole. *J. Asian Earth Sci.* **2020**, *195*, 104353. [CrossRef]
19. Bin, W.; Sun, D.S.; Chen, Q.C. Stress-state differences between sedimentary cover and basement of the Songliao basin, NE China: In-situ stress measurements at 6–7 km depth of an ICDP scientific drilling borehole (SK-II). *Tectonophysics* **2020**, *777*, 228–337.
20. Xu, M.; Li, Y.L.; Hou, H.S.; Wang, C.; Gao, R.; Wang, H.; Han, Z.; Zhou, A. Structural characteristics of the Yilan-yitong and Dunhua-mishan faults as northern extensions of the Tancheng-lujiang fault zone: New deep seismic reflection results. *Tectonophysics* **2017**, *706–707*, 35–45. [CrossRef]
21. Liu, X.F.; Zhong, G.F.; Yin, J.Y.; He, Y.; Li, X. GIS-based modeling of secondary hydrocarbon migration pathways and its application in the northern Songliao basin, China. *Comput. Geosci.* **2008**, *34*, 1115–1126. [CrossRef]
22. Liang, H.D.; Gao, R.; Hou, H.S.; Liu, G.X.; Han, J.T.; Han, S. Lithospheric electrical structure of the great Xing'an range. *J. Asian Earth Sci.* **2015**, *113*, 501–507. [CrossRef]
23. Wang, B.D.; Wang, L.Q.; Chung, S.L.; Chen, J.L.; Yin, F.G.; Liu, H.; Li, X.B.; Chen, L.K. Evolution of the Bangong-Nujiang Tethyan ocean: Insights from the geochronology and geochemistry of mafic rocks within ophiolites. *Lithos* **2016**, *245*, 18–33. [CrossRef]
24. Zhou, Z.; Yan, Y.P.; Ren, S.M.; Jiang, C.; Liu, G.; Yin, J. Prospects and strategy for shale oil exploration in Songliao basin, China. *China Min. Mag.* **2017**, *26*, 171–174.
25. Ji, Z.; Meng, Q.A.; Wan, C.B.; Ge, W.C.; Yang, H.; Zhang, Y.L.; Dong, Y.; Jin, X. Early Cretaceous adakitic lavas and a-type rhyolites in the Songliao basin, NE China: Implications for the mechanism of lithospheric extension. *Gondwana Res.* **2019**, *71*, 28–48. [CrossRef]
26. Li, C.L.; Cui, R.H.; Liu, Y.Z. Comprehensive geophysical prediction method of basement lithology-example of Binbei area, Songliao basin. *Chin. J. Geophys.* **2011**, *54*, 491–498. (In Chinese)
27. Wang, B.D.; Chen, J.L.; Xu, J.F.; Wang, L.Q. Geochemical and Sr-Nd-Pb-Os isotopic compositions of Miocene ultrapotassic rocks in southern Tibet: Petrogenesis and implications for the regional tectonic history. *Lithos* **2014**, *208–209*, 237–250. [CrossRef]
28. Wang, B.D.; Wang, L.Q.; Chen, J.L.; Yin, F.G.; Wang, D.B.; Zhang, W.P.; Chen, L.; Liu, H. Triassic three-stage collision in the Paleo-Tethys: Constraints from magmatism in the Jiangda–Deqen–Weixi continental margin arc, SW China. *Gondwana Res.* **2014**, *26*, 475–491. [CrossRef]
29. Wang, T.T.; Ramezani, J.; Wang, C.S.; Wu, H.; He, H.; Bowring, S.A. High-Precision U-Pb geochronologic constraints on the late Cretaceous terrestrial cyclostratigraphy and geomagnetic polarity from the Songliao basin, northeast China. *Earth Planet. Sci. Lett.* **2016**, *446*, 37–44. [CrossRef]
30. Wang, B.D.; Wang, L.Q.; Chen, J.L.; Liu, H.; Yin, F.G.; Li, X. Petrogenesis of Late Devonian-Early Carboniferous volcanic rocks in northern Tibet: New constraints on the Paleozoic tectonic evolution of the Tethyan Ocean. *Gondwana Res.* **2017**, *41*, 142–156. [CrossRef]
31. Zhu, Y. *Tangent and Diagram Methods for Analysis of Dip Magnetized Models*; Geological Publishing House: Beijing, China, 2012. (In Chinese)
32. Oldenburg, D.W. The inversion and interpretation of gravity anomalies. *Geophysics* **1974**, *39*, 526–536. [CrossRef]
33. Parker, R.L. The rapid calculation of potential anomalies. *Geophys. J. R. Soc.* **1973**, *31*, 447–455. [CrossRef]
34. Li, Y.G.; Oldenburg, D.W. 3-D inversion of gravity data. *Geophysics* **1998**, *63*, 109–119. [CrossRef]
35. Li, Y.G.; Oldenburg, D.W. Rapid construction of equivalent sources using wavelets. *Geophysics* **1998**, *75*, 51–59. [CrossRef]
36. Al-Zoubi, A.; Eppelbaum, L.; Abueladas, A.; Ezersky, M.; Akkawi, E. Methods for removing regional trends in microgravity under complex environments: Testing on 3D model examples and investigation in the Dead Sea coast. *Int. J. Geophys.* **2013**, *2013*, 341797. [CrossRef]
37. Eppelbaum, L.V. *Geophysical Potential Fields: Geological and Environmental Applications*; Elsevier: Amsterdam, The Netherlands, 2019; 467p.